

SCIENTIFIC REPORTS



OPEN

The mRNA capping enzyme of *Saccharomyces cerevisiae* has dual specificity to interact with CTD of RNA Polymerase II

Akhilendra Pratap Bharati¹, Neha Singh¹, Vikash Kumar¹, Md. Kashif¹, Amit Kumar Singh¹, Priyanka Singh¹, Sudhir Kumar Singh¹, Mohammad Imran Siddiqi¹, Timir Tripathi² & Md. Sohail Akhtar¹

Received: 06 May 2016

Accepted: 15 July 2016

Published: 09 August 2016

RNA Polymerase II (RNAPII) uniquely possesses an extended carboxy terminal domain (CTD) on its largest subunit, Rpb1, comprising a repetitive Tyr₁Ser₂Pro₃Thr₄Ser₅Pro₆Ser₇ motif with potential phosphorylation sites. The phosphorylation of the CTD serves as a signal for the binding of various transcription regulators for mRNA biogenesis including the mRNA capping complex. In eukaryotes, the 5' prime capping of the nascent transcript is the first detectable mRNA processing event, and is crucial for the productive transcript elongation. The binding of capping enzyme, RNA guanylyltransferases to the transcribing RNAPII is known to be primarily facilitated by the CTD, phosphorylated at Ser₅ (Ser_{5p}). Here we report that the *Saccharomyces cerevisiae* RNA guanylyltransferase (Ceg1) has dual specificity and interacts not only with Ser_{5p} but also with Ser_{7p} of the CTD. The Ser₇ of CTD is essential for the unconditional growth and efficient priming of the mRNA capping complex. The Arg159 and Arg185 of Ceg1 are the key residues that interact with the Ser_{5p}, while the Lys175 with Ser_{7p} of CTD. These interactions appear to be in a specific pattern of Ser_{5p}Ser_{7p}Ser_{5p} in a tri-heptad CTD (YSPTS_pPS YSPTSPS_pYSPTS_pPS) and provide molecular insights into the Ceg1-CTD interaction for mRNA transcription.

Eukaryotic mRNAs are transcribed by RNA polymerase II (RNAPII) and the pre-mRNAs undergo several processing events such as 5' prime (5') capping, splicing, polyadenylation etc. before becoming the mature mRNA. The 7-methyl guanosine (m7G) capping by the RNA guanylyltransferase is the first co-transcriptional modification of mRNA occurs, when the transcript is only 25–30 nucleotides long. The 5' capping helps preventing mRNA decay and play a distinct role during the mRNA biogenesis^{1,2}.

In *Saccharomyces cerevisiae*, the heterodimeric capping enzyme complex, RNA guanylyltransferase (Ceg1) and RNA triphosphatase (Cet1) are directly recruited to the carboxy-terminal domain (CTD) of Rpb1, the largest subunit of RNAPII^{3–5}. The CTD is a highly conserved unusual domain consisting of repeating heptapeptide consensus sequence (Tyr₁Ser₂Pro₃Thr₄Ser₅Pro₆Ser₇), whose copy number generally varies with the organism complexity, such as protozoa containing 15, budding yeast 26, and humans 52 repeats^{1,2}. The functional unit of CTD is di-heptapeptide and minimum 11 repeats are required for the unconditional viability in budding yeast^{6,7}. The CTD was primarily known to be phosphorylated at Ser₂ (Ser_{2p}) and Ser₅ (Ser_{5p}). These two phosphorylations were considered essential for recruiting factors important for the activity of RNAPII during mRNA biogenesis^{1,2}. Of late the Ser₇ phosphorylation was also identified during the transcription of snRNA and mRNA. Although its function is obscure in budding yeast, it contributes to the expression of noncoding RNA and mRNA splicing in mammalian cells^{1,8–11}. The phosphorylation of Ser₇ is dependent on Ser₅ phosphorylation however, the Ser₂ and Ser₅ phosphorylation is not dependent on Ser₇ phosphorylation⁸.

The CTD may undergo dynamic and combinatorial epigenetic phosphorylations (Ser₂, Ser₅ and Ser₇) with its minimal presence or enrichment at given position of the gene. The “CTD code” hypothesizes that the sequential

¹Molecular and Structural Biology Division, CSIR-Central Drug Research Institute, Sector 10, Jankipuram Extension, Lucknow, PIN 226 031, India. ²Molecular and Structural Biophysics Laboratory, Department of Biochemistry, North-Eastern Hill University, Shillong, PIN 793022, India. Correspondence and requests for materials should be addressed to M.S.A. (email: sohail@cdri.res.in)

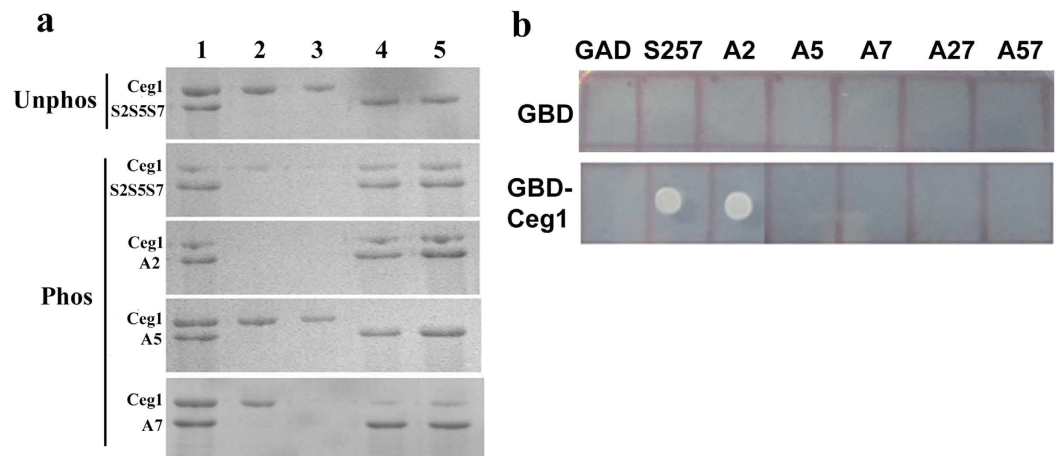


Figure 1. Ceg1 interacts with the phosphorylated Ser₅ and Ser₇ of CTD. (a) SDS PAGE analysis of the pull down assay where Ceg1 does not bind to the unphosphorylated CTD, but binds to the CTD phosphorylated by Kin28. In the first panel, lane 1 represents the purified Ceg1 (5 μg) incubated with an equal amount of unphosphorylated CTD, lane 2 and 3 represents the washed samples and Lane 4 and 5 represents the samples eluted after the extensive wash of the complex. The subsequent panel (top to bottom) represents pull down complex for CTD phosphorylated at all the three serines (S2S5S7), S5S7, S2 and S2S5 respectively. (b) Yeast two hybrid assays, where GAD vector (pGADCU-1) alone or the GAD vector expressing either the consensus CTD with all the three Ser residues (Ser₂Ser₅Ser₇ or S257) or Ser mutants (Ser₂ mutant [A2] or Ser₅ mutant [A5] or Ser₇ mutant [A7] or Ser₂ + Ser₇ double mutant [A27] or Ser₅ + Ser₇ double mutant [A57]) was co-transformed into pJ69-4A strain either with GBD vector (pGBDCU-1) alone or GBD-Ceg1. The profiles show the growth due to the transcription of a HIS3 reporter, resulting from the interaction between two-hybrid fusion proteins.

modifications of the CTD marks specify a recognition code similar to the histone code¹. A distinct pattern of all the serine phosphorylations is observed in the protein-coding genes and the role for Ser_{7p} in mRNA transcription is consistent with the observation that highly transcribed genes show high levels of this mark². The actual phosphorylation pattern and sequence in CTD, which promote protein binding or dissociation or regulate their function remains unknown *in vivo*. Furthermore, the studies on the CTD phosphorylation and function majorly relied on the use of commercial antibodies whose validity remains a subject of great debate⁹. Thus we are dealing with a situation that hinders the in depth understanding of the properties and function of CTD *in vivo*.

The phosphorylation of Ser₅ of CTD by Kin28/Cdk7 results in the coordinated recruitment of the mRNA capping complex consists of Ceg1-Cet1^{4,5}. The physical interaction between the Ser_{5p} of CTD and Ceg1 is suggested to be required for the efficient formation of 5' m7G-capping of mRNA^{12,13}. The RNA guanylyltransferases are conserved throughout the evolution and contain two domains, a nucleotidyl transferase (NT) domain and a C-terminal oligonucleotide binding (OB) domain^{4,14}. The phosphorylated CTD interacts directly with the NT domain of Ceg1, but facilitates guanylation only in the presence of Cet1^{3,4,15}. The crystal structure of *Candida albicans* RNA guanylyltransferase (Cgt1) bound to a 17 amino acid CTD phosphopeptide shows a saddle shaped CTD binding surface containing CTD docking sites (CDS) or pockets where Ser_{5p} is anchored. The Lys152, Arg157 and Tyr165 of CDS1 observed to interact with Ser_{5p} through electrostatic and hydrogen bond interaction, whereas the Arg140, Lys178 and Lys193 interact from CDS2 and make similar interactions¹⁴. The CTD content is similar in the budding yeast and bimorphic fungus *Candida albicans*. The complementation experiment, where the physiological role of individual mutations of probable CDS residues suggests that no single amino acid is essential for *ceg1* Δ cell growth. However, R157 of Cgt1 has shown a detrimental growth defect¹⁴.

Here we report the dual specificity of Ceg1, which not only interacts with Ser_{5p} but also with Ser_{7p} of CTD. We also report the residues of Ceg1 and their nature of interaction with Ser_{5p} and Ser_{7p} of CTD. The interaction between CTD and Ceg1 appears to be in a Ser₅Ser₇Ser₅ manner in order to facilitate an efficient mRNA capping.

Results

Ceg1 interacts with both Ser_{5p} and Ser_{7p} of CTD. The phosphorylation of Ser₅, primarily by the TFIIH-associated kinase Kin28, enhances the association of CTD with the m7G mRNA capping machinery^{16,17}. However, Kin28 also phosphorylates Ser₇ of CTD (only on the prephosphorylated Ser₅ heptad) and the role of this phosphorylation in mRNA transcription remains obscure^{2,8,9}. Since Kin28 marks both, the Ser₅ and Ser₇ phosphorylation at the 5' end of the gene and also the occupancy profile of Ser_{5p} and Ser_{7p} overlaps in most of the cases in this region, the role of dual phosphorylation of CTD either in Ceg1 recruitment and subsequent role in mRNA capping cannot be ruled out. In a pull down assay, an interaction between Ceg1 and the CTD phosphorylated at Ser₅ and Ser₇ (by Kin28) was observed (Fig. 1a). The Ceg1 did not show any interaction with unphosphorylated CTD (CTD-unphos) or CTD phosphorylated only at Ser₂ (A5) and was washed away before the elution (Fig. 1a, first and fourth panel). However, an interaction between Ceg1 and CTD was observed in cases where either all the three serines or at least two serines (Ser₅ and Ser₇) were phosphorylated (Fig. 1a, second and third panel). A compromise in the binding of Ceg1 with CTD was observed in cases where only Ser₇ was mutated (Fig. 1a, fifth

panel). The compromise in the efficient binding between Ceg1 and CTD in the absence of Ser_{7P} suggests that a specific and more prominent interaction exists between the Ceg1 and Ser_{5P} (Fig. 1a, fifth panel).

We subsequently verified the interaction of Ceg1 with Ser_{5P} and Ser_{7P} of CTD by carrying out a modified yeast two hybrid (Y2H) analysis, where a phosphorylation dependent binding of Ceg1 to the CTD was observed¹⁷. The binding of Ceg1 to the consensus CTD (having all the three serines) or CTD with single or double point mutations for Ser was analyzed by Y2H (Fig. 1b). The cells expressing GBD-Ceg1 (Ceg1 cloned downstream to Gal4 binding domain) grew on medium lacking Ura, Leu and His, when co-expressed with GAD-CTD (CTD cloned downstream to Gal4 activation domain) containing either all the three conserved serines in a heptad (Ser2Ser5Ser7 or S2S5S7 or S257) or at least have the Ser₅ and Ser₇ conserved (A2). On similar experimental condition the absence of growth in case of CTD mutants (A5, A7, A27 and A57) indicates the lack of significant interactions between GBD-Ceg1 and GAD-CTDs for the reporter gene expression. The absence of reporter gene expression, especially in the case of A7, clearly suggests an important role of Ser₇ in the binding of mRNA capping enzyme to CTD.

Since Ceg1 is already known to interact with Ser_{5P} of CTD for mRNA capping, its further interaction with Ser₇ appears as a stabilizer or a place keeper to increase the specificity of the interaction. This is supported by the fact that the mutation of Thr₄ and Ser₇ residues of the budding yeast (by replacing the CTD of budding yeast with that of *Mastigamoeba invertens* which contains 25 heptads of YSPASPA) shows compromise in the growth¹⁸.

Ser7 mutation affects mRNA transcription. The phosphorylation of promoter bound RNAPII-CTD by Kin28 is thought to play a critical role in the transcription initiation, promoter clearance and enhancing 5' capping of the nascent transcripts^{1,2}. The chemical inhibition of the analog sensitive Kin28 (Kin28-as) leads to the reduction in 5' capping of transcripts and steady state mRNA levels¹⁴. However, these events were primarily thought of the consequence of the reduction in the Ser_{5P} of CTD near promoter of the gene. To see the effect of the role of Ser₇ phosphorylation in mRNA transcription, we constructed CTD mutant where the Ser₇ was substituted for Ala (RNAPII-CTD-Ser₇Ala or S7A). The mutation of Ser₇ to Ala, decreased the growth of strain relative to the wild type and suggests that this mutation does not support the unconditional growth and have a role in gene regulation (Fig. 2a). To check the effect of Ser₇ phosphorylation on 5' mRNA capping, the capped mRNA transcripts from the budding yeast strain containing consensus (WT) or mutated Ser₇ (S7A) were immunoprecipitated and the level of m⁷G capping was quantified using H20, an anti-5' cap monoclonal antibody (Fig. 2b). To affirm the observation, we also checked the effect of Ser₇ mutation in fission yeast with mutated S7A construct¹⁹. Here too, the S7A affects the growth and mRNA capping similar to that observed in the budding yeast (Fig. 2c,d). The above studies affirm the role of Ser₇ phosphorylation as a place keeper to help efficient priming of 5' mRNA capping complex in yeast.

Arg159 and Arg185 of Ceg1 interacts strongly with CTD. To analyze the residues involved in the interaction between Ceg1 and phosphorylated CTD, we aligned the conserved nucleotidyl transferase (NT) domain of Ceg1 with the co-crystal structure of Cgt1 bound with a 17 amino acid of CTD sequence (TS_pPSYSPTS_pPSYSPTS_pP) phosphorylated at Ser₅ on each heptad using UCSF Chimera (Fig. 3a). We carried out the structural alignment and observed that, both the proteins exhibit a similar structural pattern, but relatively different surface electrostatic potential (Fig. 3b,c). Contrary to clustered positive patches in Cgt1, both dispersed and clustered positive patches are present in Ceg1, depicting a different binding properties for the phosphorylated CTD in *S. cerevisiae*. The residues Arg159, Arg185 and Lys198 of Ceg1 were observed to make direct contacts with Ser_{5P} (at position 2 and 16 of the peptide) in the superimposed structure model. These three residues are also conserved in Cgt1 (Fig. 3d). Out of two other electropositive residues (Lys175 and Lys179), which appears to make contact with CTD peptide, Lys175 is in close proximity to Ser₇ (at position 11) of second heptad (Fig. 3a).

To the residues of Ceg1, observed to make a possible interaction with CTD, a point mutation was created for Arg159 (Ceg1_{R159A}), Lys175 (Ceg1_{K175A}), Arg185 (Ceg1_{R185A}) and Lys198 (Ceg1_{K198A}) and the pull down assay was carried out at similar condition as described above with CTD phosphorylated by Kin28 (Fig. 4a). The mutants Ceg1_{R159A} and Ceg1_{R185A} lost interaction with CTD and was washed away before elution. However, Ceg1_{K175A} and Ceg1_{K198A} did not lose interaction with CTD and were detected in the eluent. We further checked the binding efficiency of Ceg1_{R159A} and Ceg1_{R185A} with commercial CTD peptide phosphorylated at Ser₅ by doing fluorescence anisotropy assay (Fig. 4b). The titration of phospho peptide (YSPTS_pPS-YSPTS_pPS-YSPTS_pPS) with increasing concentrations of protein shows preferential binding of Ceg1 to Ser_{5P} as compared to the mutants Ceg1_{R159A} and Ceg1_{R185A}. The observed K_d for Ceg1, Ceg1_{R159A} and Ceg1_{R185A} were ~460.7 μM, ~2373 μM and ~2285 μM respectively suggests that the residues Arg159 and Arg 185 of Ceg1 makes a significant interaction with Ser_{5P} of CTD.

To confirm the *in vivo* efficiency of Ceg1 and its mutants in binding to the CTD, a yeast two hybrid analysis was carried out as described above (Fig. 4c). We checked the binding of GBD-Ceg1, GBD-Ceg1_{R159A}, GBD-Ceg1_{K175A}, GBD-Ceg1_{R185A} and Ceg1_{K198A} with the consensus GAD-CTD fusion *in vivo*. The cells expressing GBD-Ceg1, GBD-Ceg1_{K175A} and GBD-Ceg1_{K198A} grew on medium lacking Ura, Leu and His, when co-expressed with GAD-CTD. However, cells expressing GBD-Ceg1_{R159A} and GBD-Ceg1_{R185A} did not grow optimally on similar media indicating the lack of significant interactions with GAD-CTD *in vivo*.

The above studies suggest a strong interaction between the Ser_{5P} of CTD and Arg159 and Arg185 of Ceg1. Since, the interaction of Ceg1 to phosphorylated CTD is primarily determined by phosphorylated Ser₅, the supportive interaction with Lys175 of Ceg1 was not expected to completely block the interaction between pCTD and Ceg1. The strong interaction is provided by the arginine residue in both CDS1 and CDS2. In CDS1, Arg159 provides the major stabilizing interaction, which came out as crucial residue in our *in vitro* as well as *in silico* studies. In CDS2, along with K198, Arg147 and Arg185 are two important residues, which interact strongly with phosphorylated serine. Due to presence of Arg147 and Arg185, role of K198 in CTD binding appears negligible. In the fluorescence competitive assay, the K_d for Ceg1 or Ceg1_{K175A} or Ceg1_{R198A} was also almost same.

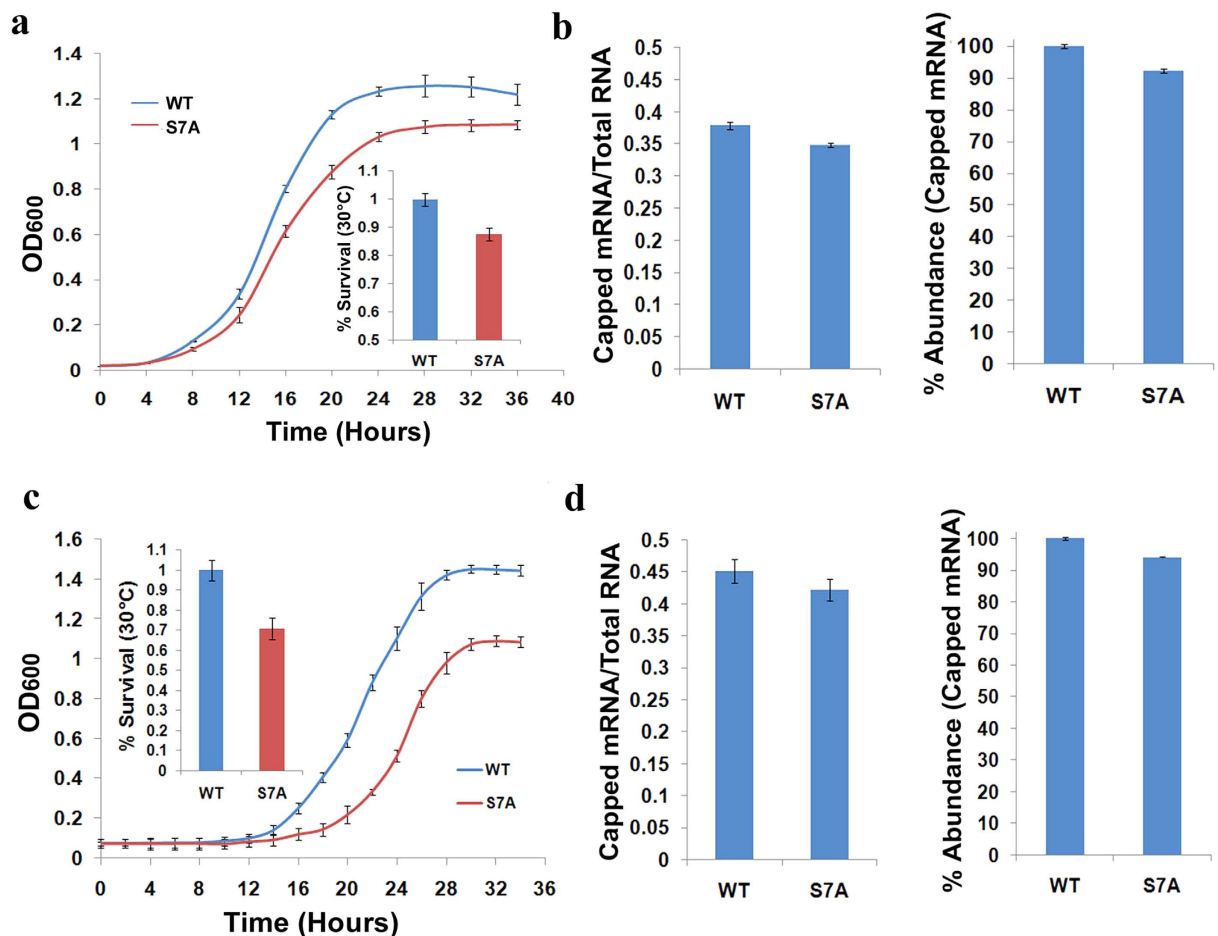


Figure 2. Ser7 mutation affects the unconditional growth and reduces the mRNA transcript capping. (a) Growth curves and the relative change in the growth for *S. cerevisiae* containing consensus (WT) and mutated (S7A) CTD heptad at 30 °C. (b) S7A reduces mRNA transcript capping. The fractional decrease in capped mRNA as well as its relative abundance was measured by doing immunoprecipitation experiment using five micrograms of RNA and H2O, an anti-5' cap monoclonal antibody. The standard deviations are displayed as error bars. (c) Growth curves and the relative change in the growth for *S. pombe* containing full length consensus (WT) and mutated (S7A) CTD heptad at 30 °C. (d) S7A reduces mRNA transcript capping. The fractional decrease in capped mRNA as well as its relative abundance in S7A as mentioned above.

MD simulations reveal a pattern of interaction between Ceg1 and CTD. The structure of CTD is very flexible and can adopt multiple conformations. The dynamic phosphorylation patterns of CTD in the transcription cycle undergo significant changes from initiation to termination, however the exact phosphorylation pattern *in vivo* remains unknown till date²⁹. It was reported that there may be only a single phosphorylation per heptad repeat (YSPTSPS), however few recent studies suggests a coexistence of Ser₂ and Ser₇ phosphorylation on the same heptad repeat⁹. It is known that the Ser₅ phosphorylation by Kin28 primes the phosphorylation of Ser₇, and hence there is almost a negligible possibility of the coexistence of Ser_{5p} and Ser_{7p} on the same heptad repeat *in vivo*^{10,20}. It is very likely that these two phosphorylation marks are on the two different heptad repeats. It is also supported by the study, where an interaction between Ser_{5p} of different heptad (position 2nd and 16th) and Cgt1 was observed in the co-crystal structure of Cgt1 bound with the TS_pPS-YSPTSP_pPS-YSPTSP_pP. In the co-crystal structure, the Ser₇ of the middle repeat (position 11) appears to be accessible to the binding by Lys175. Furthermore, the complementation experiment shows the compromised growth in case of R157 of Cgt1 (the corresponding amino acid in *S. cerevisiae* is R159) or for the double and triple point mutations in the residues from CDS1 and CDS2¹⁴. The above observations hint a possible pattern of binding between the residues of the mRNA capping enzyme (from different CDS) and phosphorylated CTD.

In order to understand the structural aspects of the Ceg1-CTD interaction, MD simulation studies were carried out. We used the available Cgt1-CTD co-crystal structure to generate the 3D-models of CTD with different phosphorylation patterns. We first extracted the coordinates of 17 amino acid long phosphorylated CTD from the Cgt1-CTD crystal structure and missing residues at the N-terminal and C-terminal were further added. After generation of 21 amino acid long three CTD heptads (three YSPTSPS motif is termed here as heptad a, b and c respectively), we carried out *in silico* phosphorylation of Ser residues in a 5a7b5c (YSPTSP_pPS-YSPTSP_pPS-YSPTSP_pPS or

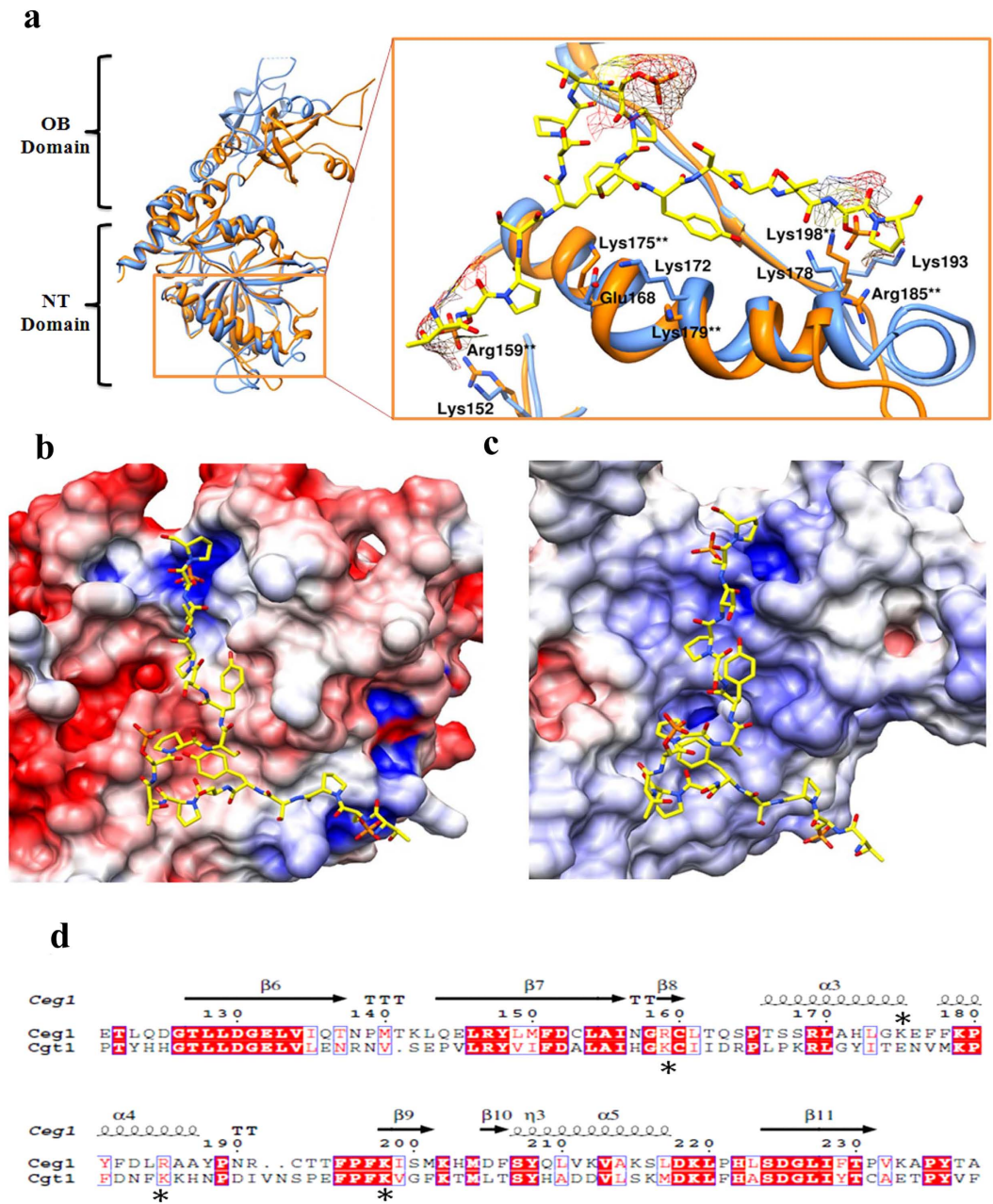


Figure 3. Structural superimposition shows key residues of Ceg1 interact with the phosphorylated CTD. (a) The superimposition of the crystal structure of Cgt1 (sky blue) and Ceg1 (orange) with an enlarged region, shows the CTD binding region where **indicates the residues from Ceg1 interacting with phosphorylated CTD. (b) The surface electrostatic potential of the NT domain complex of Cgt1 with phosphorylated CTD sequence show clustered positive patches in the form of two pockets (c) The surface electrostatic potential of the NT domain complex of Ceg1 with phosphorylated CTD sequence however shows dispersed and clustered positive patches. (d) Sequence alignment of the residues of NT domain of Ceg1 and Cgt1. Residues in the red background are fully conserved and residues in red colour are semi conserved. Symbol (*) represents the location where mutations were carried out.

CTD1) and 7a5b7c (YSPTSPS_p-YSPTSP_pPS-YSPTSPS_p or CTD2) manner. The Ceg1-CTD complexes were subsequently subjected to initial 15 ns MD simulation. The MD studies with the modeled CTD1 and CTD2 were used to get a structural and dynamic view of the Ceg1-CTD interaction as well as the conformational plasticity of the CTD. Simulation result suggests that both the CTD and CID (CTD interacting domain) exhibits an induced fit mechanism to maximize the interaction. Here CTD1 showed strong association with the Ceg1 (Fig. 5a). Residues of Ceg1 which showed interaction with CTD1 were Arg159, Arg147, Lys175, Arg185 and Arg198. The Arg159 is located in the CDS1 and is the only positively charged residue which showed interaction with the Ser_{5p} of the first heptad (a). The Arg147, Lys198 and Arg185 are located in CDS2 and showed the H-bond and electrostatic

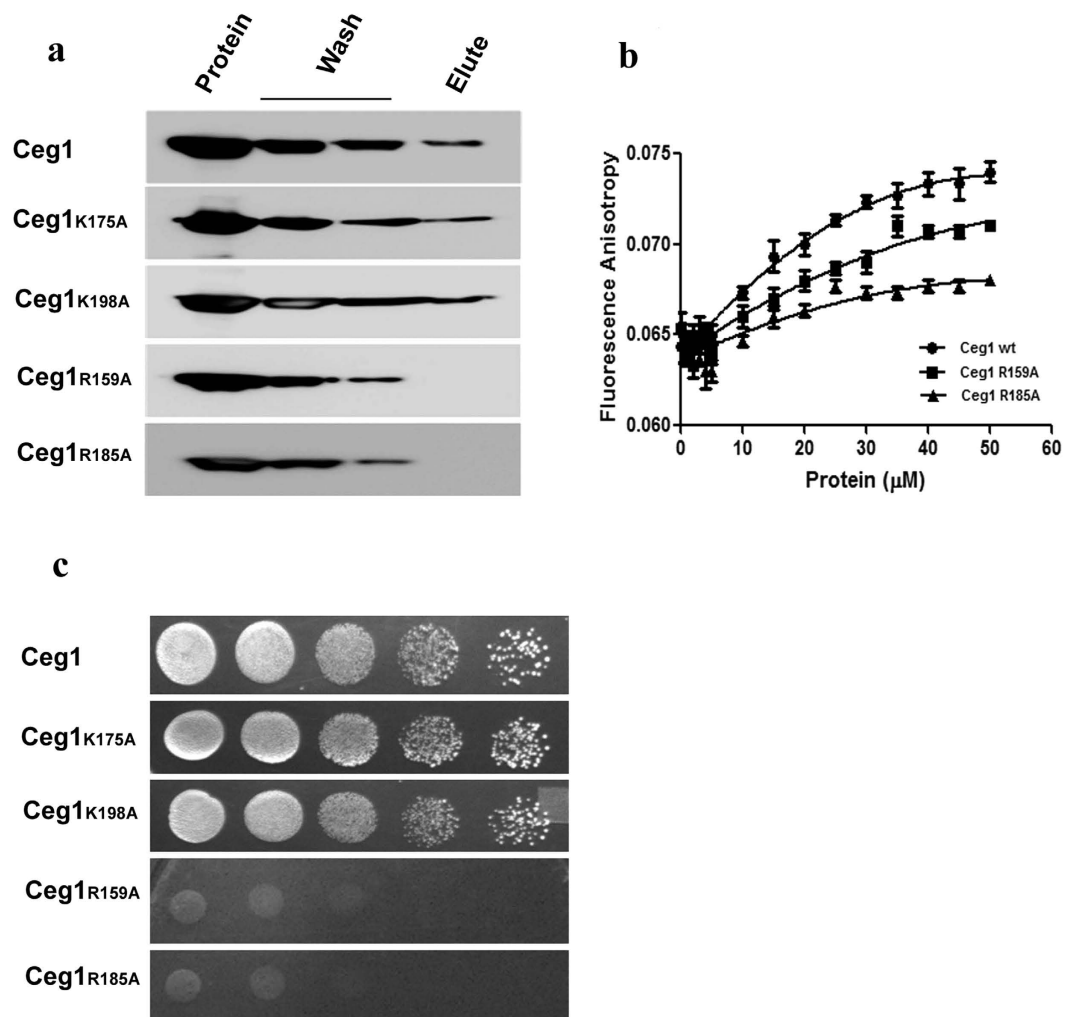


Figure 4. Arg159 and Arg185 of Ceg1 makes strong interaction with Ser_{5p} of CTD. (a) Immunodetection (anti-his) of the pull down sample where his-tagged Ceg1 or Ceg1 mutants (first lane) were incubated with CTD (14 repeats) phosphorylated by the Kin28 for their possible interaction. The samples were washed (two middle lanes) and subsequently the eluents were analyzed for the presence of Ceg1 or its mutants bound to the phosphorylated CTD (last lane). (b) The fluorescence anisotropy measurements, where 2 μM of FAM-CTD-Ser_{5p} peptide was titrated against increasing concentrations of Ceg1 (●), Ceg1^{R159A} (■) and Ceg1^{R185A} (▲) respectively to find out their binding efficiency. (c) Yeast two hybrid assays, where GAD-CTD was co-transformed into pJ69-4A strain either with GBD-Ceg1 or with Ceg1 mutants (GBD-Ceg1^{K175A} or GBD-Ceg1^{K198A} or GBD-Ceg1^{R159A} or GBD-Ceg1^{R185A}). The profiles show the growth due to the transcription of a HIS3 reporter, resulting from the interaction between two-hybrid fusion proteins.

interactions with Ser₅ of the third heptad (c). In case of Cgt1, Ser_{5p} makes extensive interaction with the two flanking sites of CID (CDS1 and CDS2), but not with the middle (14). However, in Ceg1, we see that Ser_{7p} can interact with the Lys175 residue. The presence of Lys175 residue makes the middle region of CID of Ceg1 more electropositive than the Cgt1. CTD2 also showed interaction with the Ceg1 (Fig. 5b). The Ser₇ of first heptad (a) and Ser₅ of second heptad (b) showed interaction with Lys175. None of the residues of CTD2 showed an interaction with crucial Arg159. This pattern of binding is not supported by our above mentioned *in vitro* and *in vivo* data. Backbone RMSD trajectory for Ceg1-CTD2 shows that the conformation of CTD2 is not stabilized even after 15 ns of simulation. This conformation showed higher RMSD than the Ceg1-CTD1 complex (Fig. 5c). The comparative H-bond occupancy analysis of the complexes also suggest that the Ceg1 interacts more strongly with the CTD1 than CTD2 (Fig. 6). The side chains of Arg159 showed the strong H-bond with the phosphorylated Ser5a of CTD1, while this interaction was absent in case of CTD2. The above results suggest an interaction between Ceg1 and CTD1 with more specificity for Ser5aSer7bSer5c (S5S7S5) manner.

Since CTD1 showed better interaction with Ceg1, we further carried out a separate long (55ns) MD simulation studies of CTD1 bound to NT domain of Ceg1 (1–242) (Fig. 7a). C α -RMSD trajectory showed that the Ceg1-CTD1 complex is stable during the MD simulation. Here, with increase in the simulation length, CTD1 appeared to interact more strongly with the Ceg1. The phosphorylated Ser7b showed extensive interaction with Lys114 and Lys179 (Fig. 7b,c). The above results suggest an interaction between Ceg1 and CTD1 with more specificity

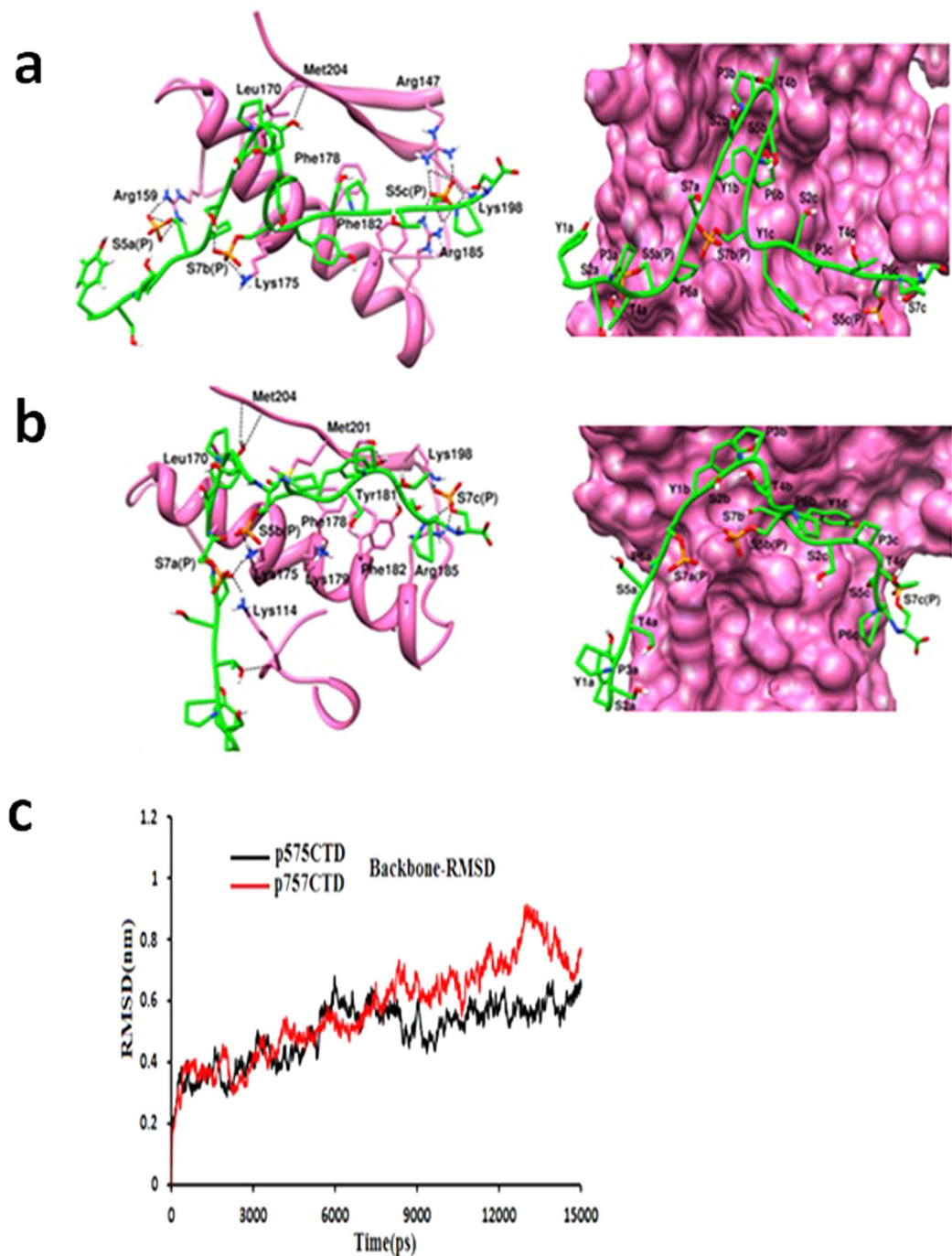


Figure 5. Phosphorylated CTD heptad shows a specific interaction pattern with Ceg1. (a) The left panel shows the interaction profile of CTD1 (YSPTS_pPS-YSPTS_pPS-YSPTS_pPS) with Ceg1-CID, obtained after 15 ns MD simulation. The right panel shows the surface view of Ceg1-CID (hot pink) with CTD1. H-bonds are shown in black dotted line. For clear representation only polar hydrogens are shown. (b) The right panel shows the interaction profile of CTD2 (YSPTS_pPS-YSPTS_pPS-YSPTS_pPS) with Ceg1-CID, obtained after 15 ns MD simulation. The right panel shows the surface view of Ceg1-CID (hot pink) with CTD2. (c) Root mean square deviation of the backbone atoms of Ceg1-CTD1 (black) and Ceg1-CTD2 (red) complexes.

for 5a7b5c (YSPTS_pPS-YSPTS_pPS-YSPTS_pPS) manner. Using MD simulation studies, we have also investigated the effect of Ceg1_{R185A} and Ceg1_{K198A} mutations on CTD1 binding. Since the cells bearing Ceg1_{R185A} mutation did not grow optimally, we speculated that the loss of interaction between phosphorylated Ser₅c and Ceg1_{R185A} will have significant impact on CTD1 binding. In case of Ceg1_{R185A}, CTD1 adopts a different conformation on the CID surface as compared to Ceg1 (Fig. 6b), and phosphorylated Ser₅ of third heptad showed interaction with Arg147 and Lys198. In addition, phosphorylated Ser₅ of first heptad and Ser₇ of second heptad showed interaction

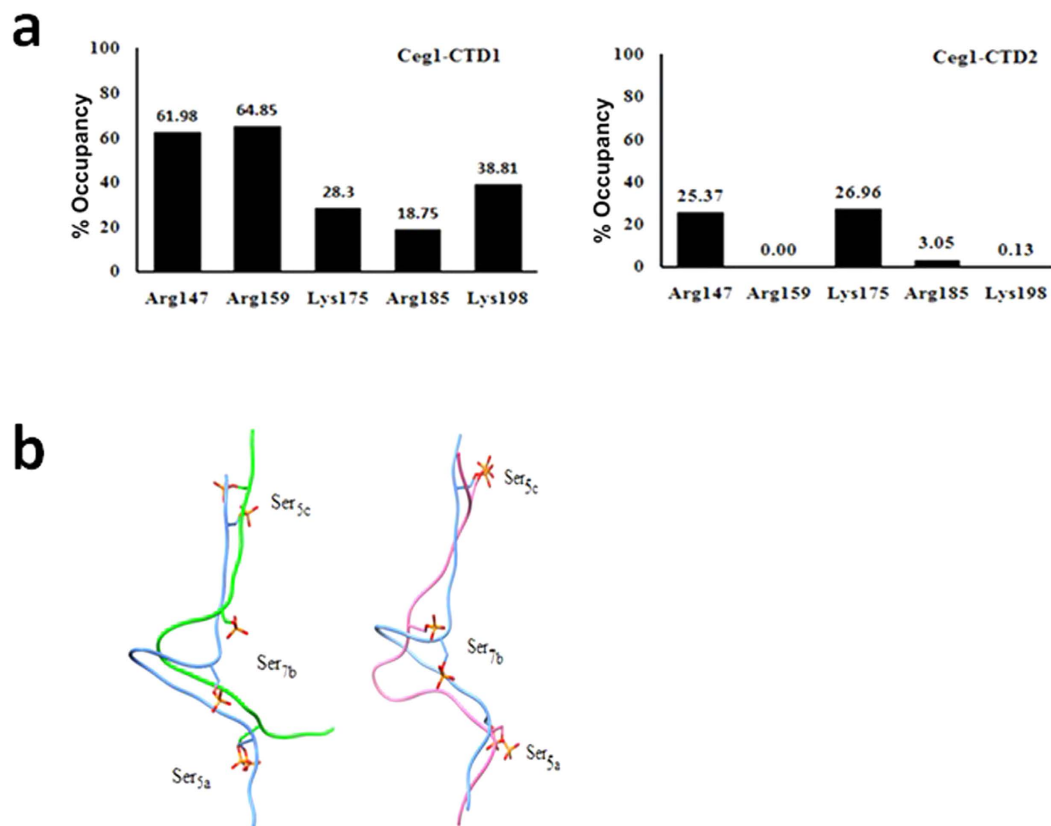


Figure 6. Ceg1 interacts more strongly with CTD1. **(a)** H-bond occupancy plot during 15ns of MD simulation for Ceg1-CTD1 (left panel) and Ceg1-CTD2 (right panel). **(b)** The left panel shows the superimposed CTD1 conformations in case of Ceg1 (blue) and Ceg1_{R185A} (green) after 15ns of MD simulation. The right panel shows the superimposed CTD1 conformation in case of Ceg1 (blue) and Ceg1_{K198A} (pink) at similar condition.

with Arg159 and Lys175 respectively. The hydrophobic/hydrophilic interactions analysis shows a compromised hydrophobic interaction between Ceg1_{R185A} and CTD1. For Ceg1, Ceg1_{R185A} and Ceg1_{K198A}, the areas of lipophilic surface matches with CTD1 were of 89.30 Å², 16.52 Å² and 63.73 Å² respectively. In case of Ceg1_{K198A}, CTD1 maintained the hydrophobic interaction and the loss of hydrophobic interaction for Ceg1_{R185A}, appears to affect the CTD1 binding (Table 1). It has been reported that Tyr and Pro residues in CTD repeat are involved in hydrophobic interaction with the CID⁹ and hence the contribution of hydrophobic interaction in CTD-Ceg1 interaction cannot be ruled out. The binding of CTD1 with Ceg1_{R185A} was further investigated by carrying out a separate 55 ns MD simulation (Figs 7a and 8a). The CTD1 showed a similar interaction pattern as explained in the previous 15ns MD simulation (Fig. 8b). We observed that in both 15 ns and 55 ns of MD simulation, CTD1 adopt different conformations in Ceg1-CTD1 and Ceg1_{R185A}-CTD1 (Fig. 8c). The calculations obtained from the PLATINUM and PDBePISA servers reveal that in case of Ceg1_{R185A}, there is a significant decrease in the binding affinity for CTD1 (Tables 1 and 2).

Discussion

The presence of Ser₇ at the most degenerate position in CTD heptads (appearing 26/52 in human, 7/24 in *drosophila*, 19/26 in yeast) suggests its specialized function^{1,2}. This is supported by the fact that the presence of only consensus CTD repeats (52 repeats with YSPTSPS) in mammals shows reduced growth compared to the wild type cells²¹. The current knowledge of CTD based transcription progression of mRNA is mostly based on the phosphorylation at Ser₂ and Ser₅. Lately identified Ser_{7p} and the presence of this mark as observed by ChIP and ChIP chip signals at 5' end, middle and 3' end of the protein coding genes, makes the whole transcription cycle more complicated and dynamic. It further suggests that the role of Ser_{7p} is not limited to the snRNA transcription only. In addition to the probable specialized function of this mark, the combinatorial possibility of the differential phosphorylation and its subsequent function also cannot be ruled out. As evident, the integrator recruitment to CTD was found to be influenced by Ser_{2p} + Ser_{7p} double mark during snRNA transcription²². Hence, it is too preliminary to conclude that the different transcription regulators bind due to specifically phosphorylated Ser₂ and/or Ser₅ only.

The non-homologous Ser₅ mutations of CTD are synthetically lethal. In *Saccharomyces cerevisiae*, the Cet1-Ceg1 complex is thought to be recruited to Ser_{5p} of CTD^{3,4,6}. In the process of establishing the interaction between Ceg1 and CTD, a role of Ser₇ has always been overlooked due to the fact that this phosphorylation was not known at the time of studies being carried out on the Ceg1-CTD interaction and its subsequent role in the

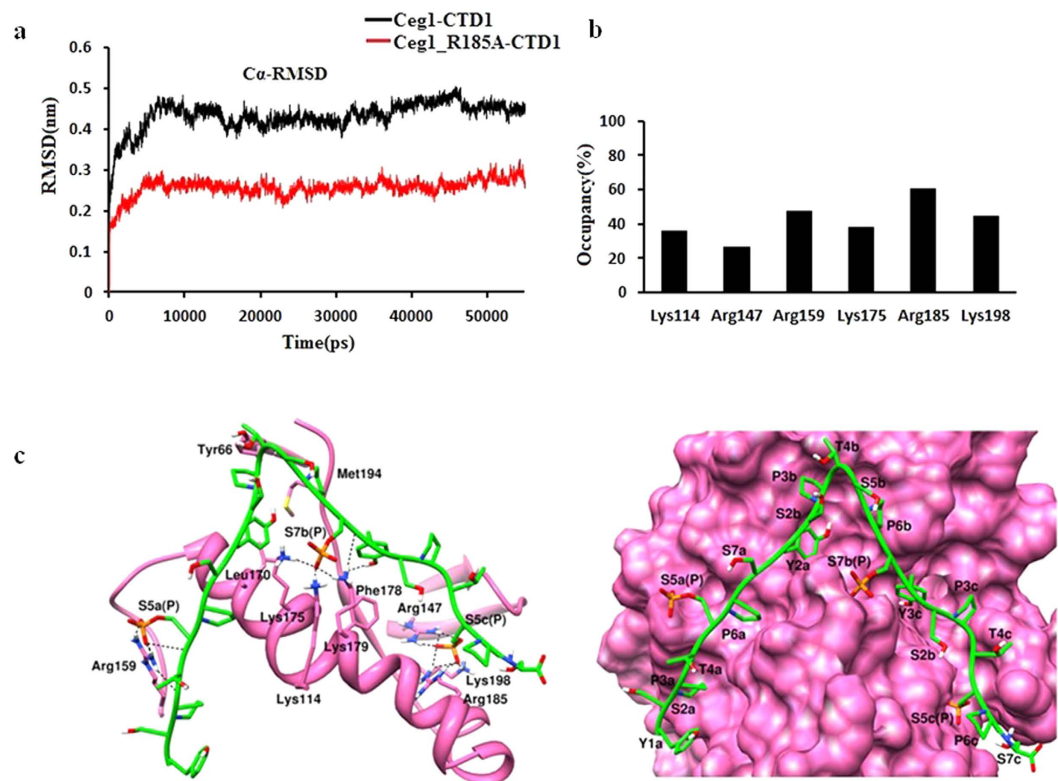


Figure 7. MD simulation of Ceg1-CTD1 and Ceg1_{R185A}-CTD1. (a) C α -RMSD of Ceg1-CTD1 and Ceg1_{R185A}-CTD1 calculated over 55 ns MD simulation. (b) The occupancy of H-bonds formed between CTD1 and Ceg1. (c) Left panel shows interaction of CTD1 with Ceg1 and the right panel shows the conformation of CTD1 over the surface of Ceg1.

Ligand	#H-bonds	S(L/L)	S(H/H)	S _{buried}	S _{total}	Match ¹	Match ²
WtCeg1-CTD1	(9.57)	(99.05)	(523.33)	(861.38)	(1878.89)	(0.3360)	(0.3195)
	9.42	89.30	391.13	650.18	1754.01	0.2739	0.3305
Ceg1R185A-CTD1	(8.11)	(83.73)	(329.99)	(517.40)	(1818.31)	(0.2275)	(0.3360)
	10.12	16.52	409.36	725.68	1827.38	0.2331	(0.0702)
Ceg1K198A-CTD1	8.09	63.73	412.40	675.11	1808.20	0.2461	0.2461

Table 1. The hydrophobic/hydrophilic interaction analysis using PLATINUM tool (www.model.nmr.ru/platinum). S(L/L), S(H/H), S_{buried}, S_{total}, Match¹, Match² represent an area of lipophilic match surface (Å²), hydrophilic match surface (Å²), ligand buried surface (Å²), total surface area (Å²), fraction of matching total surface (Å²) and fraction of matching hydrophobic surface (Å²) respectively. Values in brackets are obtained after analysis of last frame obtained after 55 ns MD simulation.

mRNA capping or other similar studies. The *in vitro* pull down, and yeast two hybrid analysis with mutant CTD suggests the interaction of Ceg1 with CTD. The observed effect of Ser₇ mutation on the growth and mRNA capping suggests its role beyond snRNA transcription and of biological significance. The insignificant change in the mRNA capping due to Ser₇ mutation suggests the role as one among many which could influence the mRNA transcription. The major possibilities are of its role being as a place keeper for other CTD binding proteins which inadvertently affects different process of transcription¹⁹. The structural superimpositions of Ceg1-CTD and Cgt1-CTD identifies key residues of budding yeast mRNA capping enzyme, having potential to interact with Ser₅ and Ser₇ of CTD. The absence of significant interaction between Lys175 of Ceg1 and CTD is attributed for the strong preferential binding with Ser_{5p} of alternate CTD heptad and hence the Ser_{7p} appears to act as a place keeper residue. The MD simulation studies of Ceg1 with a tri-heptad CTD phosphorylated as 5a7b5c (YSPTSP_p-YSPTSPS_p-YSPTSP_p) manner supports the interaction of Arg159, Lys175 and Arg198 in the given manner. Our studies explore the role of Ser₇ phosphorylation in mRNA transcription and also show a pattern of CTD phosphorylation not described before for the recruitment of mRNA capping enzyme.

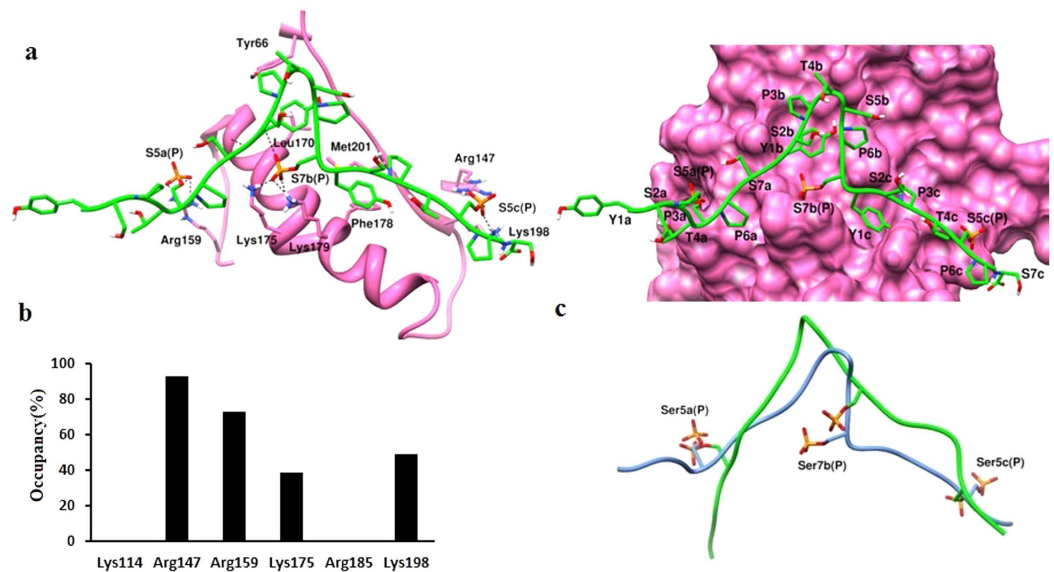


Figure 8. The mutation R185A alters the interaction of CTD1 with Ceg1. (a) Left panel shows an interaction between CTD1 and Ceg1_{R185A}. The right panel shows the conformation of CTD1 over the surface of Ceg1_{R185A}. (b) H-bond occupancy analysis of Ceg1_{R185A}-CTD1 interaction. (c) The aligned conformations of CTD1 with Ceg1 (green) and Ceg1_{R185A} (blue). For the interaction analysis, the last frame obtained after 55 ns MD simulation was used.

Ligand	N _{HB}	Interface area (Å ²)	Δ ⁱ G (Kcal/mol)
Ceg1-5a7b5c	15	1256.6	-24.2
Ceg1 _{R185A} -5a7b5c	9	720.8	-14.7

Table 2. Interface analysis using PDBePISA server (www.ebi.ac.uk/pdbe/pisa/).

Methods

Cloning, expression and purification of Ceg1 and mutants. *ceg1* gene was PCR amplified from the genomic DNA of *S. cerevisiae* (S288C) using primer pair 5′CTAGCTAGCATGGT ATTGGCA ATGGAAAGT AGAGTGGCA-3′ and 5′-ATAAGAATGCGGCCGCGTCAGACCAATCATCCTCAT CTA-3′. PCR conditions used were: 94 °C-5 min; 94 °C-1 min; 61 °C-1 min, 72 °C-1 min (30 cycles); 72 °C-10 min. The amplified fragments were digested with NheI and NotI and then ligated into the pET-21d (+) vector (Novagen) cut with the same enzymes. Competent DH5-α cells were transformed with the plasmid constructs and screened for positive clones. The mutants Ceg1_{R159A}, Ceg1_{K175A}, Ceg1_{R185A} and Ceg1_{K198A} were generated from the above construct using the GeneTailor™ Site-Directed Mutagenesis System (Invitrogen) and the mutagenic primer pairs ATCAACGGTGCCTGTCTCACACAATCACCA/GTGAGACACGCACCGTTGAT AGCAAGACA,CACCTTGGAGCGGATTTTTTAAACCATAC/AAAAAATTCGGCTCCAAGGTGGGCTAG TCT,TTCGATTTAGCGGCAGCGTACCCTAATCGT/GTACGCTGCCGCTAAATCGAAGTATG GTTT,TTCCGTTCCGCGATTTCCATGAAACATATG/CATGGAAATCGCGAACGGAAAAGTAGTACA respectively. The conditions used for amplification were same as specified for use with Platinum Pfx DNA polymerase (Invitrogen). The mutants (Ceg1_{R159A}, Ceg1_{K175A}, Ceg1_{R185A} and Ceg1_{K198A}) for over expression were cloned in pET-21d (+). Two hybrid plasmids pGBDU-C1 and pGAD-C1 code for the DNA binding (GBD) and transcriptional activation (GAD) domains of Gal4p respectively, and the construction of GBD-Ceg1, GAD-S2S5S7, GAD-A2S5S7 and GAD S2A5S7 have been described previously^{23,24}. The mutants for the two hybrid analysis (GBD-Ceg1_{R159A}, GBD-Ceg1_{K175A}, GBD-Ceg1_{R185A} and GBD-Ceg1_{K198A}) were cloned using TCCCCGGGATGGTATTGGCAATGGAAAGTAGAGTGGCA/GAAGATCTCG GCCGCG TCAGACCAATCATCCTCATCTA primer pairs. Sequences containing the mutated CTD repeats (14 heptads), S2S5A7, A2S5A7 and S2A5A7 were custom synthesized from IDT and cloned into pGAD-C1 vector as described previously²⁴. The DNA sequencing of all the amplified genes confirmed the sequence homogeneity.

The BL21 (DE3) expressing Ceg1 or its mutant (all his-tagged) was inoculated into 500 ml of LB broth having ampicillin (100 μg/ml) and allowed to grow at 37 °C until A₆₀₀ of 0.6 was achieved. The culture was then induced with 0.5 mM IPTG and incubated further at 37 °C for 4 hours. The cells were harvested and the resultant pellet was resuspended in lysis buffer containing 50 mM Tris Cl (pH 8), 100 mM NaCl and 2 mM PMSF and disrupted using a probe-type ultrasonicator followed by high speed centrifugation for 30 min at 4 °C. The supernatant was loaded onto the Ni NTA column, washed and eluted using 300 mM imidazole. The GST-CTD was purified and kinase assay was performed as described previously^{8,25}.

Fluorescence anisotropy. Measurements were carried out in a fluorescence spectrometer in T-configuration (Perkin Elmer LS50b) in buffer (25 mM HEPES pH-8, 100 mM NaCl, 1 mM EDTA, 1 mM DTT) at 25 °C as described previously²⁶. For binding experiments, Ceg1 or mutants were titrated into a reaction mixture containing buffer supplemented with 2 μ M of FAM-CTD-Ser_{sp} (YSPTS_pPS-YSPTS_pPS-YSPTS_pPS). Data were fitted to the cubic equation applying nonlinear regression one site total binding mode as described in GraphPad Prism 5.

Pull down assay. The GST-CTD was incubated for 4 hours at 4 °C with equilibrated glutathione beads in 20 mM HEPES-KOH (pH-7.3), 15 mM magnesium acetate, 100 mM potassium acetate, 1 mM DTT, 2.5 mM EGTA and 10% glycerol. After washing, the GST-CTD was phosphorylated by Kin28²⁵, washed and incubated with Ceg1 or its mutants for overnight at 4 °C. The reaction mixture was extensively washed to remove the unbound proteins, before elution with reduced glutathione. In case of mutant analysis, after pull down assay the proteins were transferred onto nitrocellulose membrane and Ceg1 detected using anti his antibody.

MD simulation. MD simulation studies were carried out with the help of Gromacs 4.5.5²⁷. The Cgt1-CTD co-crystal structure was used to generate the 3D-models of CTD with different phosphorylation patterns (14). The Biopolymer module of SYBYLX-2.0 was used to generate 21 amino acid CTD heptad and subsequent phosphorylation of Ser residues using the phosphorylate tool²⁸. To preserve the crystal conformation of CTD, the energy minimization on the generated peptides were not carried out. The generated CTD repeats were then positioned on the mapped CTD interaction interface of Ceg1 using the structural alignment method available in UCSF Chimera1.6²⁹. Each of Ceg1-CTD complexes was subjected to MD simulation under Gromos43a1 forcefield³⁰. The SPC water model was used to solvate the complexes in the periodic cubic box. Na⁺ and Cl⁻ ions were added to neutralize the systems at a concentration of 0.1 M. After minimization of solvated systems, NVT and NPT equilibration were carried out for 500 ps and 1 ns respectively. The temperature of the system was maintained at 300 K. Finally, systems were subjected to 15 ns production simulation.

Yeast two hybrid. Two-hybrid plasmids pGBDU-C1 and pGAD-C1 code for the DNA binding (GBD) and transcriptional activation (GAD) domains of Gal4p, respectively (15). Two hybrid plasmids pGAD-S2S5A7 (14 repeats), pGAD-A2S5A7 (14 repeats), pGAD-S2A5A7 (14 repeats), were constructed by fusing mutant DNA sequences coding for the CTD of Rpb1 to DNA coding for transcriptional activation domain of Gal4p in pGAD-C1. Sequences containing the mutated CTD repeats were custom synthesized from IDT. The assay was performed by transforming the strain PJ69-4A with different GAD plasmids to the Ceg1-GBD and their growth was assayed on synthetic drop-out medium containing appropriate amino acids supplemented with 2% glucose. Growth on lacking medium is due to the expression of the reporter gene (HIS3) by the interaction of the two hybrid fusion proteins fused upstream of the DNA binding (GBD) and transcriptional activation (GAD) domains of Gal4p. A 10 μ l aliquot of serial 10-fold dilutions were spotted on sc-ura-leu-his plates and photographed after incubation at 30 °C for 36 hours.

RNA Immunoprecipitation. The experiment was performed as described previously³¹. Briefly, yeast strain with consensus and with Ser7A mutant (14 repeats) were grown at 30 °C and harvested at mid log phase for RNA isolation. Protein A/G plus agarose beads were washed three times with 1.5 ml of buffer IPP150 (150 mM NaCl/0.1% Nonidet P40/10 mM Tris, pH 8.0) and three times with 1.25 ml of buffer IPP500 (500 mM NaCl/0.1% Nonidet P40/10 mM Tris, pH 8.0) and resuspended in 100 μ l of buffer IPP500/reaction. H20 antibody (5 μ g per reaction) was added and rotated at 4 °C overnight on a tube rotator to couple the beads to the antibody. H20 antibody recognizes the 2,2,7-trimethylguanosine (m3G) containing cap structure. After coupling, the beads were washed three times with IPP150 and resuspended in the IP reaction mix (5 μ g of total RNA, DTT, RiboLock RNase Inhibitor and IPP150 buffer up to a total volume of 200 μ l). Mock IP reaction with no antibody served as nonspecific binding control. IP reactions were rotated at 4 °C overnight. The beads were washed five times in 1 ml of cold IPP150 containing 2.5 mM DTT and resuspended in 200 μ l of Proteinase K solution and put on a tube rotator at 37 °C for 30 min to recover the RNA from the pellet. Then 200 μ l of IPP150, 20 μ l of glycogen (10 mg/ml) and 400 μ l of acid phenol:chloroform were added to each sample. RNA was extracted by vortexing for 15 seconds and spinning for 5 min at maximum speed and room temperature. After ethanol precipitation, the RNA pellets were resuspended in DEPC treated water. mRNA capping experiments was performed exactly as described previously³².

References

- Buratowski, S. Progression through the RNA polymerase II CTD cycle. *Mol. Cell.* **36**, 541–546 (2009).
- Zhang, D. W. *et al.* Emerging views on the CTD code. *Genet. Res. Int.* p 347214 (2012).
- Cho, E. J. *et al.* Allosteric interactions between capping enzyme subunits and the RNA polymerase II carboxy-terminal domain. *Genes Dev.* **12**, 3482–3487 (1998).
- Gu, M. *et al.* Structure of the *Saccharomyces cerevisiae* Cet1-Ceg1 mRNA capping apparatus. *Structure.* **18**, 216–227 (2010).
- Shuman, S. What messenger RNA capping tells us about eukaryotic evolution. *Nat. Rev. Mol. Cell Biol.* **3**, 619–625 (2002).
- Liu, P. *et al.* The essential sequence elements required for RNAP II carboxyl-terminal domain function in yeast and their evolutionary conservation. *Mol. Biol. Evol.* **25**, 719–727 (2008).
- Corden, J. L. RNA polymerase II C-terminal domain: tethering transcription to transcript and template. *Chem. Rev.* **113**, 8423–8455 (2013).
- Akhtar, M. S. *et al.* TFIIH kinase places bivalent marks on the carboxy-terminal domain of RNA polymerase II. *Mol. Cell.* **34**, 387–393 (2009).
- Eick, D. & Geyer, M. The RNA polymerase II carboxy-terminal domain (CTD) code. *Chem. Rev.* **113**, 8456–8490 (2013).
- Suh, H. *et al.* Direct analysis of phosphorylation sites on the Rpb1 c-terminal domain of RNA polymerase II. *Mol. Cell.* **61**, 297–304 (2016).
- Egloff, S. *et al.* Serine-7 of the RNA polymerase II CTD is specifically required for snRNA gene expression. *Science* **318**, 1777–1779 (2007).

12. Cho, E.-J. *et al.* mRNA capping enzyme is recruited to the transcription complex by phosphorylation of the RNA polymerase II carboxy-terminal domain. *Genes Dev.* **11**, 3319–3326 (1997).
13. McCracken, S. *et al.* 5'-Capping enzymes are targeted to pre-mRNA by binding to the phosphorylated carboxy-terminal domain of RNA polymerase II. *Genes Dev.* **11**, 3306–3318 (1997).
14. Fabrega, C. *et al.* Structure of an mRNA capping enzyme bound to the phosphorylated carboxy-terminal domain of RNA polymerase II. *Mol. Cell* **11**, 1549–1561 (2003).
15. Shuman, S. & Lima, C. D. The polynucleotide ligase and RNA capping enzyme superfamily of covalent nucleotidyltransferases. *Curr. Opin. Struct. Biol.* **14**, 757–764 (2004).
16. Komarnitsky, P. *et al.* Different phosphorylated forms of RNA polymerase II and associated mRNA processing factors during transcription. *Genes Dev.* **14**, 2452–2460 (2000).
17. Schroeder, S. C. *et al.* Dynamic association of capping enzymes with transcribing RNA polymerase II. *Genes Dev.* **14**, 2435–2440 (2000).
18. Stiller, J. W. *et al.* Evolutionary complementation for polymerase II CTD function. *Yeast* **16**, 57–64 (2000).
19. Schwer, B. & Shuman, S. Deciphering the RNA polymerase II CTD code in fission yeast. *Mol. Cell* **43**, 311–318 (2011).
20. Schüller, R. *et al.* Heptad-specific phosphorylation of RNA polymerase II CTD. *Mol. Cell* **61**, 305–314 (2016).
21. Chapman, R. D. *et al.* Transcribing RNA polymerase II is phosphorylated at CTD residue serine-7. *Science* **318**, 1780–1782 (2007).
22. Eglöf, S. *et al.* The integrator complex recognizes a new double mark on the RNA polymerase II carboxyl-terminal domain. *J. Biol. Chem.* **285**, 20564–20569 (2010).
23. James, P. *et al.* Genomic libraries and a host strain designed for highly efficient two-hybrid selection in yeast. *Genetics* **144**, 1425–1436 (1996).
24. Ursic, D. *et al.* Detecting phosphorylation-dependent interactions with the C-terminal domain of RNA polymerase II subunit Rpb1p using a yeast two-hybrid assay. *RNA Biol.* **5**, 1–4 (2008).
25. Ansari, A. Z. *et al.* Transcriptional activating regions target attached substrates to a cyclin-dependent kinase. *Proc. Natl. Acad. Sci. USA* **102**, 2346–2349 (2005).
26. Becker, R. *et al.* Snapshots of the RNA processing factor SCAF8 bound to different phosphorylated forms of the carboxyl-terminal domain of RNA polymerase II. *J. Biol. Chem.* **283**, 22659–22669 (2008).
27. Pronk, S. *et al.* GROMACS 4.5: a high-throughput and highly parallel open source molecular simulation toolkit. *Bioinformatics* **29**, 845–854 (2013).
28. Sybyl-X molecular modeling software packages, Version 2.0. TRIPOS associates, Inc; St. Louis, MO, USA: **2012**.
29. Pettersen, E. F. *et al.* UCSF chimera—a visualization system for exploratory research and analysis. *J. Comput. Chem.* **25**, 1605–1612 (2004).
30. van Gunsteren, W. F., Billeter, S. R., Eising, A. A., Hünenberger, P. H. & Krüger, P. Biomolecular Simulation: The GROMOS96 manual and user guide Vdf Hochschulverlag, AG Zurich, Switzerland (1996).
31. Kanin, E. I. *et al.* Chemical inhibition of the TFIIH-associated kinase Cdk7/Kin28 does not impair global mRNA synthesis. *Proc. Natl. Acad. Sci. USA* **104**, 5812–5817 (2007).
32. Kwan, S. *et al.* Disruption of the 5' stem-loop of yeast U6 RNA induces trimethylguanosine capping of this RNA polymerase III transcript *in vivo*. *RNA* **6**, 1859–1869 (2000).

Acknowledgements

This work was supported in part by BSC-0118 and BSC-0103 to M.S.A., BSC-0121 to M.I.S. and BT/224/NE/TBP/2011 to M.S.A. and T.T. A.P.B., N.S., M.K., A.K.S. and V.K. are grateful to CSIR, New Delhi for financial assistance. We thank Aseem Z. Ansari for his constant support and encouragements. We thank B. Schwer, J.L. Corden, M. Culbertson and E.A. Craig for strains and plasmids. This is CDRI communication number 9282.

Author Contributions

A.P.B., V.K., I.S. and M.S.A. conceived the idea. A.P.B., V.K., N.S., M.K., A.K.S., P.S. and S.K.S. performed experiments. A.P.B., V.K., T.T., M.I.S. and M.S.A. analyzed the data and gave critical inputs. A.P.B., V.K., M.I.S. and M.S.A. wrote the paper.

Additional Information

Competing financial interests: The authors declare no competing financial interests.

How to cite this article: Bharati, A. P. *et al.* The mRNA capping enzyme of *Saccharomyces cerevisiae* has dual specificity to interact with CTD of RNA Polymerase II. *Sci. Rep.* **6**, 31294; doi: 10.1038/srep31294 (2016).



This work is licensed under a Creative Commons Attribution 4.0 International License. The images or other third party material in this article are included in the article's Creative Commons license, unless indicated otherwise in the credit line; if the material is not included under the Creative Commons license, users will need to obtain permission from the license holder to reproduce the material. To view a copy of this license, visit <http://creativecommons.org/licenses/by/4.0/>

© The Author(s) 2016